Journal of Sound and Vibration (1997) **203**(5), 763–779

DETERMINATION OF STATISTICAL ENERGY ANALYSIS LOSS FACTORS BY MEANS OF AN INPUT POWER MODULATION TECHNIQUE

F. J. Fahy and H. M. Ruivo*

Institute of Sound and Vibration Research, University of Southampton, Southampton SO17 1BJ, England

(*Received* 21 *July* 1996, *and in final form* 18 *December* 1996)

An input power modulation technique is proposed as an alternative to the widely used steady-state power injection method for the *in-situ* determination of dissipation and coupling loss factors of subsystems selected for an SEA model of a physical system. There is no requirement to measure input power and, in principle, response measurements are made at only one point on each subsystem. Theory is developed for a two-subsystem model. An input power modulation device is described, and the loss factor estimates resulting from its application to systems comprising two structurally coupled plates and two acoustically coupled rooms are presented and compared with those from steady state tests. A phenomenon of energy response modulation phase dispersion is observed at modulation frequencies in excess of about 10 Hz.

1. INTRODUCTION

The first stage in the application of Statistical Energy Analysis to a physical system is the selection of subsystems. At present, there is little in the way of guidance or criteria to assist the SEA modeller in taking this crucial step, although efforts are currently being made to remedy this unsatisfactory situation [1]. Although rapid progress is being made in the theoretical derivation of coupling loss factors between structural components, there still exists a need for empirically derived data: to validate theoretical analysis; to determine coupling loss factor (CLF's) in cases in which theoretical estimates are unavailable; and to determine dissipation loss factors (DLF's), which generally cannot be theoretically predicted. The universally employed method for the *in situ* determination of CLF's and DLF's is based upon the sequential injection of vibrational/acoustic power into each subsystem, together with the measurement of response at a number of locations in each subsystem see [e.g. references, 2, 3]. Physical power injection may be replaced by virtual power injection derived from transfer function measurements [4].

This method has a number of drawbacks: (i) physical constraints often hinder the attachment of vibration exciters at appropriate locations; (ii) experimental estimates of input power are widely recognized to be subject to various errors which may sometimes be large and are always unknown; (iii) the power injection technique relies upon the generation of a subsystem energy matrix—but energy cannot be directly measured and must be inferred from a set of measurements of kinetic or dynamic variables at discrete points distributed over a subsystem; the associated uncertainty in the total energy can be very large indeed; (iv) an inappropriate choice of subsystems may create an ill-conditioned

* Since returned to the Brazilian Navy.

0022–460X/97/250763 + 17 $25.00/0/sv960892

energy matrix which upon inversion will produce large errors in the derived loss factors; (v) measurement errors and uncertainties in individual elements of the energy matrix are propagated throughout the predicted loss factor matrix in a very complex manner; (vi) last, but not least, for systems divided into more than about five subsystems, the power injection method is very time consuming.

Various strategies have been devised to minimize the errors of loss factor estimation associated with the power injection method [5], but the economic cost of application remains a significant deterrent to its widespread application. As a consequence, an alternative test principle has been independently proposed by Lundberg [6–8] and Fahy [9]. This paper, which is based upon an M.Sc. dissertation by Ruivo [10], explains the principle of an input power modulation technique, and presents a comparison of DLF and CLF estimates for simple two-element structural and acoustic systems derived by means of steady state and modulation techniques. Attention is also drawn to a phenomenon of energy response modulation phase dispersion which has implications for the validity of so-called "transient SEA".

2. THEORY

2.1. FUNDAMENTAL ASSUMPTION

The assumption fundamental to the following analysis, and to its practical application, is that the steady state SEA proportionality relation between the time-average rate of energy transfer (power flow) from subsystem A to subsystem B (forward power), and the time-average vibrational energy stored in subsystem A, holds when the short-time average input power and energies vary smoothly on a time scale much larger than the average period of the vibrational processes in operation. An associated implication is that the vibrational state of subsystem may be expressed in terms of a single degree of freedom, so that the temporal variation of energy density is assumed to be spatially uniform over the domain of any one subsystem. The physical implication is that energy transferred to a subsystem is diffused throughout the subsystem on a time scale much smaller than the input power modulation period.

A running short-time average value of an energetic quantity $X(t)$ is defined as

$$\langle X(t)\rangle_T = (1/T)\int_{t-T/2}^{t+T/2} X(t)\mathrm{d}t. \tag{1}$$

In this paper, for typographical simplicity, $\langle X(t)\rangle_T$ is written as $\langle X\rangle$, on the understanding that T indicates an integration (averaging) interval which is much greater than the inverse of the lowest frequency of the linear quantities which contribute to $X(t)$, but much smaller than the inverse of the imposed modulation frequency. The resulting quantity will resemble the envelope of $X(t)$.

2.2. RESPONSE OF TWO COUPLED SUBSYSTEMS TO MODULATED INPUT POWER

The subsystems are labelled 1 and 2. It is assumed that vibrational power is injected into subsystem 1 through the agency of some vibrational excitation mechanism, and that the excitation is frequency-band limited. Because the input power modulation frequencies used are two or three orders smaller than the vibrational frequencies, the modulation process causes negligible widening of this band. On the assumption that the subsystems behave linearly, their responses will be confined to the same frequency band. Hence one may use the term "band-limited input power", which, of course, does not mean that the

spectrum of the time-dependent power is so limited. It is further assumed that, by means of some hypothetical mechanism, this band-limited power is modulated harmonically at frequency 2Ω, as represented by

$$\langle P_1 \rangle = \overline{P}_1 + \tilde{P}_1 \exp(\mathrm{i}2\Omega t), \tag{2}$$

in which the tilde represents the complex amplitude of a phasor.

In accordance with the assumed linearity of the SEA power balance equations,

$$\langle E_1 \rangle = \overline{E_1} + \tilde{E}_1 \exp(\mathrm{i}2\Omega t) \qquad \text{and} \qquad \langle E_2 \rangle = \overline{E_2} + \tilde{E}_2 \exp(\mathrm{i}2\Omega t). \tag{3a, b}$$

These quantities are depicted graphically in Figure 1, in which the significant response descriptors are the normalized modulation response amplitudes, $|\tilde{E}_1|/|\tilde{P}_1|$ and $|\tilde{E}_2|/|\tilde{P}_1|$, the relative phases $\angle(\tilde{E}_1/\tilde{P}_1)$ and $\angle(\tilde{E}_2/\tilde{P}_1)$, and the relative modulation amplitudes $|\tilde{E}_1|/\overline{E_1}$ and $|\tilde{E}_2|/\overline{E_2}$.

On the basis of the fundamental assumptions stated above, the time-dependent SEA power balance equations may be written

$$\mathrm{d}\langle E_1 \rangle/\mathrm{d}t = \langle P_1 \rangle - \langle E_1 \rangle \omega(\eta_{12} + \eta_1) + \langle E_2 \rangle \omega \eta_{21}, \tag{4a}$$

$$\mathrm{d}\langle E_2 \rangle/\mathrm{d}t = \langle E_1 \rangle \omega \eta_{12} - \langle E_2 \rangle \omega(\eta_{21} + \eta_2), \tag{4b}$$

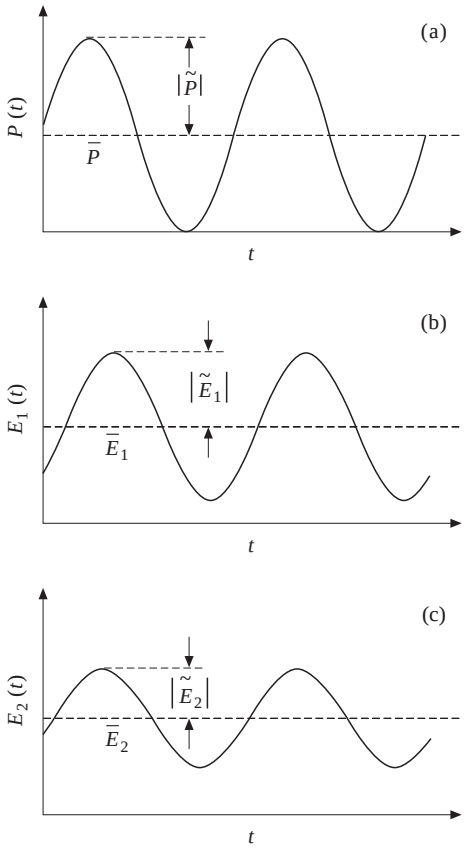

Figure 1. Envelopes of (a) input power and stored energy in (b) subsystem 1 and (c) subsystem 2.

where η_i represents DLF and η_{ij} represents CLF. Substitution of the expressions for $\langle P \rangle$ and $\langle E_i \rangle$ from equations (2) and (3) into equations (4), together with elimination of steady state averages $\bar{P}$ and $\overline{E_i}$, yields

$$\tilde{P}_1 - \tilde{E}_1\omega(\eta_{12} + \eta_1 + \mathrm{i}2\Omega/\omega) + \tilde{E}_2\omega\eta_{21} = 0, \qquad \tilde{E}_1\omega\eta_{12} - \tilde{E}_2\omega(\eta_{21} + \eta_2 + \mathrm{i}2\Omega/\omega) = 0. \tag{5a, b}$$

For simplicity of notation, the following substitutions will be employed:

$$a \equiv \eta_{12}\omega, \qquad b \equiv \eta_{21}\omega, \qquad c \equiv \eta_1\omega, \qquad d \equiv \eta_2\omega.$$

Equations (5) yield the relations

$$\tilde{E}_2/\tilde{E}_1 = a/[b + d + 2\mathrm{i}\Omega], \qquad \tilde{E}_2/\tilde{P}_1 = a/[4\Omega_0^2 - 4\Omega^2 + 2\mathrm{i}\Omega C], \tag{6a, b}$$

$$\tilde{E}_1/\tilde{P}_1 = [b + d + 2\mathrm{i}\Omega]/[4\Omega_0^2 - 4\Omega^2 + 2\mathrm{i}\Omega C], \tag{6c}$$

$$\angle(\tilde{E}_2/\tilde{E}_1) = \arctan[-2\Omega/(b + d)], \qquad \angle(\tilde{E}_2/\tilde{P}_1) = \arctan[-2\Omega C/(4\Omega_0^2 - 4\Omega^2)], \tag{6d, e}$$

$$\angle(\tilde{E}_1/\tilde{P}_1) = \arctan[2\Omega(4\Omega_0^2 - 4\Omega^2 - (b + d)C)]/[(4\Omega_0^2 - 4\Omega^2)(b + d) + 4\Omega^2 C], \tag{6f}$$

$$|\tilde{E}_1|/\overline{E_1} = [(b + d)^2 + 4\Omega^2]^{1/2}[4\Omega_0^2/(b + d)]/[(4\Omega_0^2 - 4\Omega^2)^2 + 4\Omega^2 C^2]^{1/2}, \tag{6g}$$

$$|\tilde{E}_2|/\overline{E_2} = 4\Omega_0^2/[4\Omega_0^2 - 4\Omega^2)^2 + 4\Omega^2 C^2]^{1/2}, \tag{6h}$$

in which $4\Omega_0^2 = bc + cd + ad$ and $C = a + b + c + d$.

Equation (6b) has the form of a s.d.o.f. resonant response, in which 2Ω represents the excitation frequency, $bc + dc + ad$ is equivalent to the square of the natural frequency $2\Omega_0$, and $a + b + c + d$ is equivalent to the damping ratio C. As it will turn out, this "resonant" system is normally greatly overdamped, and a resonance peak is not observed.

It is assumed that the (unknown) constant which relates the total energy of a subsystem to the short-time average of the square of a relevant response variable measured at any point on the subsystem is the same for steady state and modulated quantities; for example, the normalized modulation depth $|\tilde{E}_1|/\overline{E_1}$ may be determined from measurements at any position on subsystem 1. The modulation phase of short-time averaged subsystem energy relative to that of input power may also be determined from a response measurement at any point on the subsystem.

On the basis of this assumption, equations (6d–h) define non-dimensional quantities which may be evaluated experimentally from *single point* response measurements and *without quantitative knowledge of the absolute magnitude of the input power*. The crucial question of the validity of this fundamental assumption is explored in section 6.2.

2.3. SOLUTION OF THE RESPONSE EQUATIONS

It is not possible to solve for all the unknowns a, b, c and d from equations (6d–h). Nor can additional independent non-dimensional ratios be obtained by applying excitation to subsystem 2, since $4\Omega_0^2$ and C remain unchanged. This impasse may be overcome in two ways. If the theoretical subsystem modal density ratio n_1/n_2 is available, fundamental SEA theory shows that it may be equated to the ratio $\eta_{21}/\eta_{12} = b/a$; alternatively, multi-point response measurements may be made on each subsystem to provide an estimate of the absolute energy ratios $\overline{E_2}/\overline{E_1}$ or $|\tilde{E}_2|/|\tilde{E}_1|$; this is attended by the problem of estimating the effective subsystem masses, which is a source of considerable uncertainty in SEA experiments.

Since the need to make multi-point measurements is undesirable, the following analysis is based upon an assumption that n_1/n_2 can be estimated.

When

$$\angle(\tilde{E}_2/\tilde{E}_1) = -\Pi/4, \qquad 2\Omega = b + d. \tag{7a}$$

When

$$\angle(\tilde{E}_2/\tilde{P}_1) = -\Pi/2, \qquad 2\Omega = 2\Omega_0 = [c(b + d) + ad]^{1/2} \tag{7b}$$

and

$$|\tilde{E}_2|/\overline{E_2} = 2\Omega_0/C = 2\Omega_0/(a + b + c + d), \tag{7c}$$

from which $b + d$ and $a + c$ may be obtained.

Let $n_1/n_2 = b/a = \alpha$, $a + c = M$ and $b + d = N$. Then

$$a = [(MN - 4\Omega_0^2)/\alpha]^{1/2}, \qquad b = \alpha a, \quad c = M - a \quad \text{and} \quad d = N - \alpha a. \tag{7d, e}$$

Since $\eta_{12} \ll \eta_1$ and $\eta_{21} \ll \eta_2$ in many practical systems, the order of magnitude of the ratio of modulation "resonance" frequency $2\Omega_0$ to excitation band centre frequency ω is given by equation (7b) as $2\Omega_0/\omega \sim (\eta_1\eta_2)^{1/2}$; i.e. typically between 10^{-2} and 10^{-3}.

Although it is, in principle, possible to employ equations (7a–c) directly, it is preferable to curve-fit the measured variations with the modulation frequency 2Ω of $\angle(\tilde{E}_2/\tilde{E}_1)$, $\angle(\tilde{E}_2/\tilde{P}_1)$ and $|\tilde{E}_2|/\overline{E_2}$, expressed by equations (6c), (6f) and (6h). Equation (7d) is not well conditioned, and it will normally be necessary to measure responses at more than one point to assess the standard deviation of the estimates of η_{12} and hence of η_{21}. It would also be wise to check the sensitivity of the estimated values to the location of the power injection locations.

3. POWER MODULATION

Instantaneous power imput generated by an applied vibrational force is given by

$$P(t) = F(t)v(t), \tag{8}$$

in which v is the component of response velocity vector at the driving point which is co-linear with the force. $P(t)$ can theoretically be conditioned according to equation (2), but it contains the response quantity v and therefore can not be independently controlled.

Instead, a band-limited random input force (exciter current) was cosinusoidally modulated at frequency Ω, and squared, hence yielding a squared force modulated at frequency 2Ω about a steady mean value:

$$F(t) = (f(t)\cos\Omega t)^2 = (f^2(t)/2)\,(1 + \cos 2\Omega t). \tag{9}$$

The presence of 2Ω in this equation explains its earlier appearance in the power balance equations.

In order to make an initial attack on the fundamental question concerning the relation between $F(t)$ and $P(t)$, a simple harmonic model has been analyzed. Since it does not provide a complete answer to this question, but may provoke others to improve on it, the details have been relegated to the Appendix. The result of the analysis, plus computational simulations, suggest that the error incurred by assuming that $\langle P \rangle$ is proportional to $\langle F^2 \rangle$ may not be large, especially for subsystems having modal overlaps of unity and above.

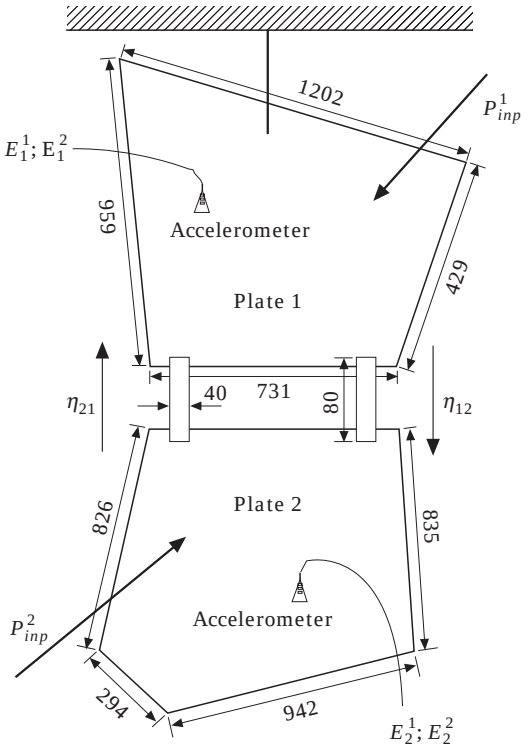

Figure 2. The geometry of coupled plates. Dimensions in mm; plate thickness = 3 mm; drawing not to scale.

4. STEADY STATE POWER INJECTION MEASUREMENTS

4.1. COUPLED PLATES

The steady state power injection method was applied to the two uniform steel plates coupled by straps of the same material shown in Figure 2; the superscript on E indicates which subsystem is directly excited. The force applied by a non-contact magnet-and-coil exciter was monitored by an interposed Brüel and Kjaer (B&K) type 8200 force transducer, and the resulting acceleration at the excitation point was monitored by means of a B&K type 4374 (0·65 g) accelerometer calibrated with a normalized standard deviation of repeatability of 1%. The nominal force transducer calibration was assumed. A broadband (100–5000 Hz) excitation signal was applied at three points on each plate and, in each case, the resulting accelerations were measured at ten points on each plate, all with a frequency resolution of 3·125 Hz and a BT product of 10. The force–acceleration coherence was very close to unity over the entire frequency range.

The plate vibrational kinetic energy densities were estimated from the acceleration spectra in 200 Hz bands over the range 400–4000 Hz. The input powers were estimated from the imaginary part of the force–acceleration cross-spectrum with a BT product of 25 [11]; this method proved to be more reliable than that based upon the measurement of the force or acceleration auto-spectra and the theoretical infinite plate mobility. The DLF's and CLF's were derived by application of the conventional technique of energy matrix inversion:

$$\omega[\eta] = [\bar{E}]^{-1}[\bar{P}]. \tag{10}$$

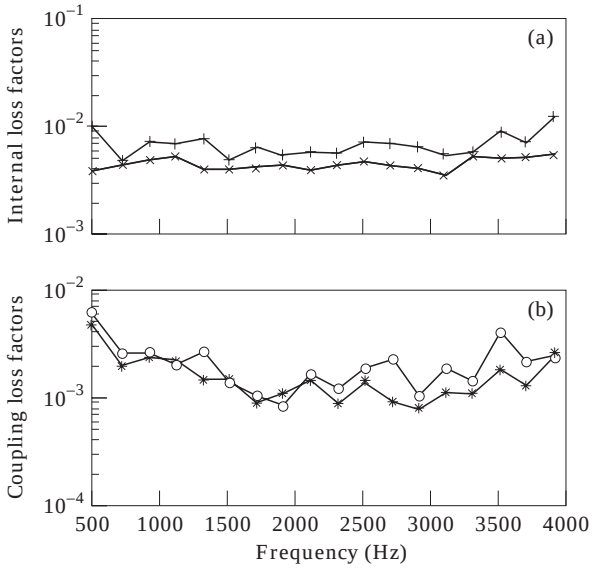

Figure 3. Loss factor estimates for coupled plates: 200 Hz bands. (a) +, η_1, ×, η_2; (b) ○, η_{12}, ∗, η_{21}.

The results are presented in Figure 3, which shows that the CLF's are generally smaller than the DLF's, a commonly accepted indicator of a state of "weak coupling". Note that damping sheets were applied to the bare plates to increase their DLF's to values more typical of practical situations. The associated modal energy spectra, which confirm the existence of weak coupling, are presented in Figure 4.

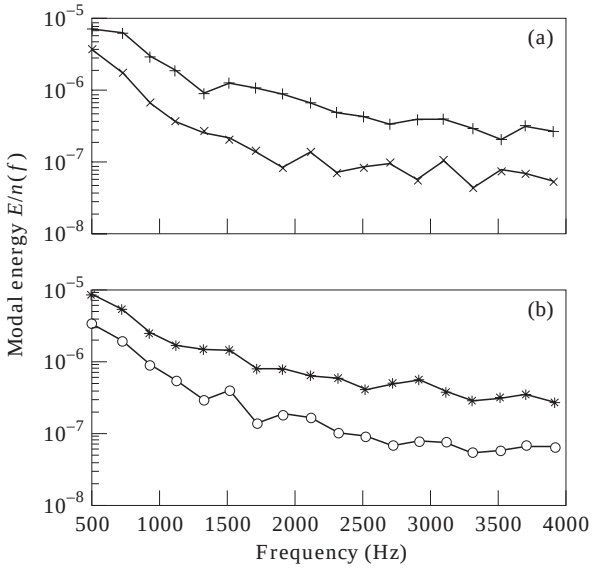

Figure 4. Modal energies of coupled plates: 200 Hz bands. (a) Input power applied to plate 1; (b) input power applied to plate 2. Modal energies: (a) + plate 1, × plate 2; (b) ○ plate 1, ∗ plate 2.

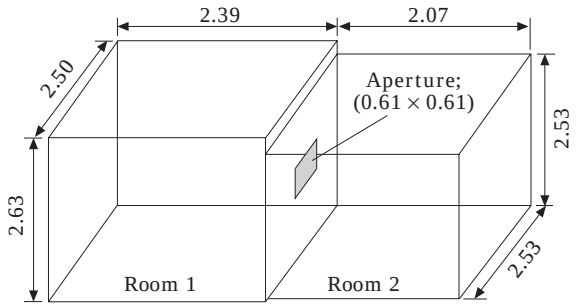

Figure 5. The geometry of coupled rooms. Dimensions in metres.

4.2. COUPLED ROOMS

The steady state power injection method was applied to two small reverberant rooms coupled by an aperture in the separating wall (see Figure 5). The power injected by a loudspeaker was determined from a sound intensity scan over an enclosing surface, using a B&K typw 3519 intensity probe (spacing 12 mm) and a B&K type 4437 sound intensity analyzer to generate sound pressure and particle velocity signals to feed to a FFT analyzer for the estimation of the cross-spectrum. Calibration was effected by a B&K type 3541 Calibrator. The estimated sound power repeatability range was typically $\pm$ 0·5 dB. Sound pressure, for the estimation of acoustic energy densities, was measured with B&K type microphones 4165 calibrated with a class 1 pistonphone, with the normal associated accuracy and precison.

The estimates of DLF's and CLF's obtained from energy matrix inversion are presented in Figure 6 and the associated modal energies are presented in Figure 7: "weak coupling" is apparent over the whole frequency range of measurement.

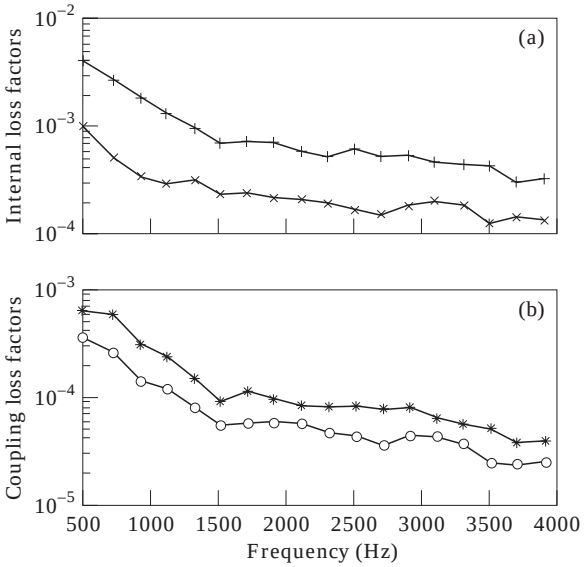

Figure 6. Loss factor estimates for coupled rooms: 200 Hz bands. (a) + η_1, × η_2; (b) ○ η_{12}, ∗ η_{21}.

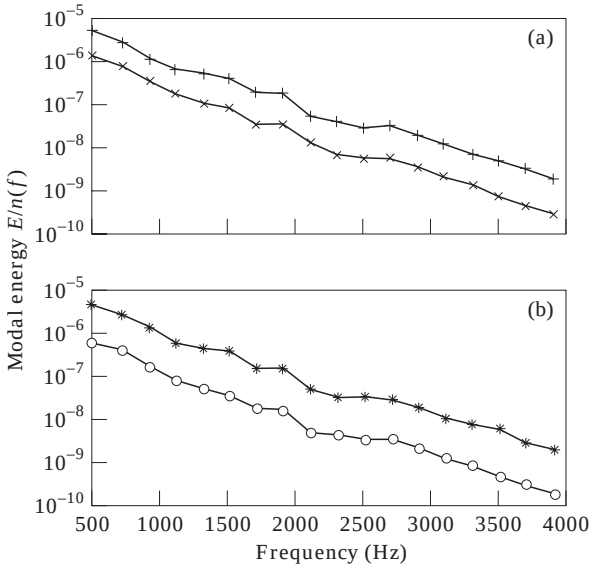

Figure 7. The modal energies of coupled rooms: 200 Hz bands. Input power applied to (a) room 1 and (b) room 2. Modal energies: (a) + room 1, × room 2; (b) ○ room 1, ∗ room 2.

5. INPUT POWER MODULATION TESTS

5.1. MODULATION EQUIPMENT

An analog electrical circuit was designed and constructed to generate signals representing input "power" and response energy. The excitation signal is multiplied by a sinusoidal signal generated by an external oscillator; the modulated signal is squared and

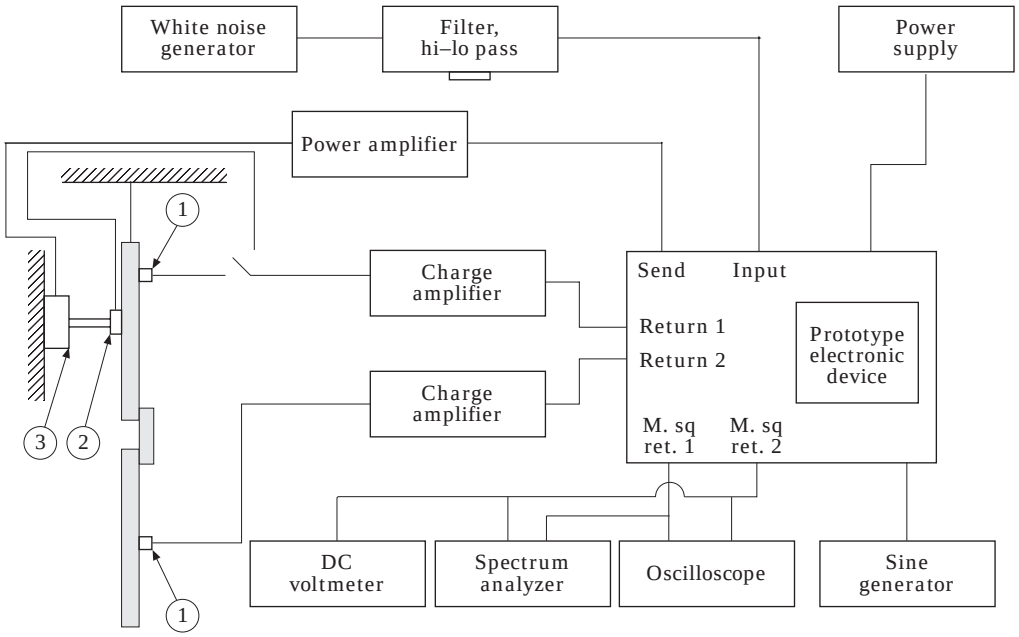

Figure 8. A schematic of modulation tests on coupled plates. (1) Accelerometer; (2) force transducer; (3) shaker.

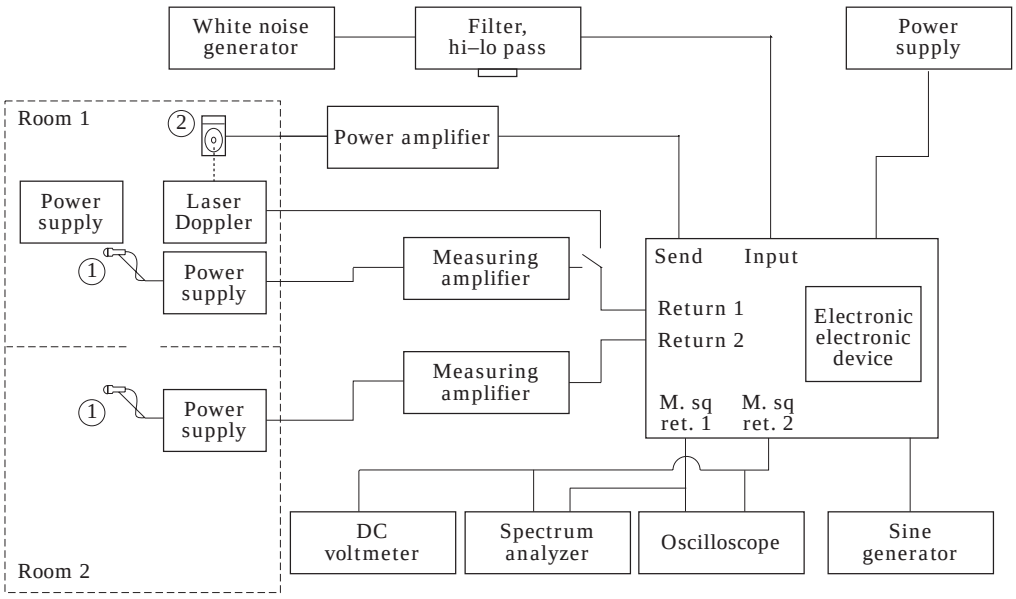

Figure 9. A schematic of modulation tests on coupled rooms. (1) Microphone; (2) loudspeaker.

smoothed by low-pass filtering to produce an approximation to its envelope. The response signals are also squared and smoothed. The device also outputs the long-time average of the squared signals. A schematic of the equipment as utilized for the plate test is shown in Figure 8 and that for the room tests in Figure 9. The phase mismatch between the envelope-generating channels was less than $\pm 1^\circ$ over the frequency range of the test.

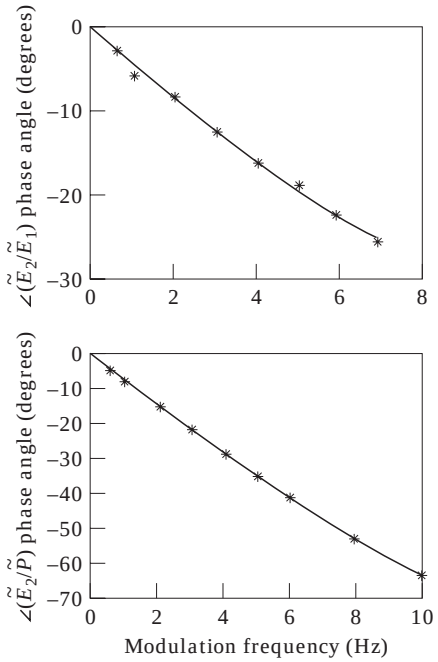

Figure 10. Examples of best-fit curves for plates.

5.2. TEST PROCEDURE

Band-pass filtered random input signals in the frequency ranges 600–800, 2400–2600 and 3800–4000 Hz were selected for comparison of loss factor estimates with those from the steady state power injection tests. Time constraints on the M.Sc. project precluded tests in a greater number of bands. Modulation frequencies were varied in steps between 0·5 and 10 Hz. At each frequency the smoothed "envelope" signals were input to an FFT analyzer which estimated the transfer function and phase at the "power" modulation frequency 2Ω, using a high resolution zoom. This frequency was easily identifiable by the dominant coherence peak of unity. The modulated signal representing the acoustic input to the reverberation rooms was derived from a Laser Doppler Velocimeter monitoring the loudspeaker cone velocity. Although not necessary in principle, response measurements were made at ten individual locations on each subsystem to investigate the degree of spatial uniformity of response modulation phase.

5.3. DATA ANALYSIS

Initial tests showed that the equations for loss factors based upon data generated by excitation of only subsystem 1 were poorly conditioned, the estimates of η_{21} and η_2 being particularly unreliable. Consequently, although not in principle necessary, input power was sequentially injected into each subsystem to improve the quality of the results. The various relations expressed by equations (6d–h) were evaluated as functions of 2Ω, and best-fit curves computed, under the constraint that the phase angles had to be zero at zero Hz (steady state). Examples are shown in Figures 10 and 11.

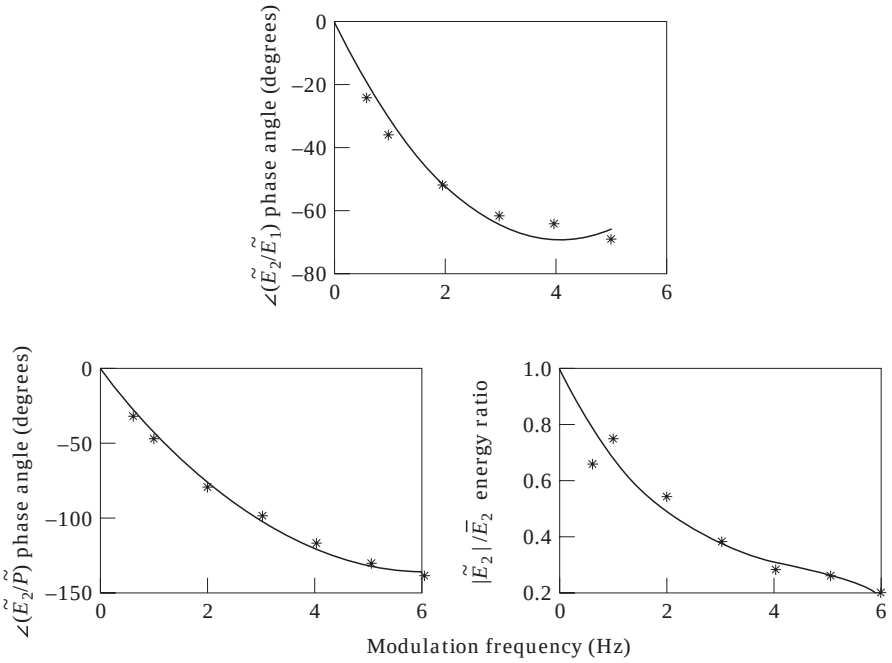

Figure 11. Examples of best-fit curves for rooms.

TABLE 1

A comparison of estimated CLF's and DLF's of coupled plates

Band centre frequency (Hz)	Loss and coupling loss factors	Values from power injection method	Values from power modulation technique	Deviation (db)
700 (U3, L10)	η_1	5·13e − 3	8·40e − 3	2.2
	η_{12}	2·44e − 3	2·60e − 3	0.3
	η_{21}	1·91e − 3	1·80e − 3	−0·2
	η_2	4·56e − 3	4·60e − 3	0
700 (U7, L8)	η_1	5·13e − 3	7·30e − 3	1·6
	η_{12}	2·44e − 3	2·40e − 3	0
	η_{21}	1·91e − 3	1·70e − 4	−0.5
	η_2	4·56e − 3	2·60e − 3	−2·5
2500	η_1	7·22e − 3	7·60e − 3	0·2
	η_{12}	1·84e − 3	1·50e − 3	−0·8
	η_{21}	1·40e − 3	1·10e − 3	−1·0
	η_2	4·85e − 3	3·90e − 3	−1·0
3900	η_1	1·27e − 2	8·50e − 3	−1·7
	η_{12}	1·43e − 3	1·20e − 3	−3·0
	η_{21}	2·50e − 3	8·18e − 4	−4·9
	η_2	5·84e − 3	4·00e − 3	−1·6

6. RESULTS

6.1. DERIVED LOSS FACTORS

The DLF's and CLF's derived from the steady state and modulation techniques are compared in Table 1 and 2. Note that results are obtained for two different pairs of points at 700 Hz for plates and 3900 Hz for rooms.

TABLE 2

As table 1, *but for coupled rooms*

Band centre frequency (Hz)	Loss and coupling loss factors	Values from power injection method	Values from power modulation technique	Deviation (dB)
700	η_1	2·77e − 3	2·40e − 3	−0·7
	η_{12}	2·72e − 4	5·17e − 4	2·8
	η_{21}	5·89e − 4	6·13e − 4	0·2
	η_2	5·43e − 4	2·30e − 3	6·3
2500	η_1	6·16e − 4	5·26e − 4	− 0·7
	η_{12}	4·48e − 5	1·06e − 4	3·7
	η_{21}	8·71e − 5	1·26e − 4	1·6
	η_2	1·72e − 4	5·60e − 4	5·1
3900 (1/1)	η_1	3·33e − 4	4·53e − 4	1·3
	η_{12}	2·55e − 5	5·60e − 5	3·4
	η_{21}	4·02e − 5	6·64e − 5	2·2
	η_2	1·40e − 4	3·12e − 4	3·5
3900 (6/6)	η_1	3·33e − 4	3·79e − 4	0·6
	η_{12}	2·55e − 5	5·87e − 5	3·6
	η_{21}	4·02e − 5	6·96e − 5	2·4
	η_2	1·40e − 4	4·42e − 4	5·0

TABLE 3

The phase dispersion of plates

Modulation frequency (Hz)	Pair of measurement locations	$\angle(\tilde{E}_2/\tilde{E}_1)$ (degrees)
1	1/1	−6
	4/4	−7
	9/9	−9
	10/10	−7
2·3	1/1	−15
	4/4	−13
	9/9	−13
	10/10	−14
5	1/1	−31
	4/4	−23
	9/9	−21
	10/10	−27
10	1/1	−58
	4/4	−23
	9/9	−33
	10/10	−40

6.2. ENERGY MODULATION PHASE DISPERSION

It was observed for both the plates and the rooms that the energy envelope response phase exhibited spatial variations which increased with modulation frequency. An example from the plate measurements is presented in Table 3. Remarkably, modification of the plate mass by 10% by the addition of ten randomly spaced magnets altered these values very little. The same phenomenon was observed in the rooms, as shown by Table 4. Measurements of the relative phases of the envelope of Cartesian components of acoustic kinetic density and of the potential energy density were also made in a room with an intensity probe and B&K 4437 intensity analyzer which outputs analog signals proportional to sound pressure and to the component of particle velocity directed along

TABLE 4

The phase dispersion of rooms

Modulation frequency (Hz)	Pair of measurement locations	$\angle(\tilde{E}_2/\tilde{E}_1)$ (degrees)
1	1/1	−32
	2/2	−33
	4/4	−29
	6/6	−35
5	1/1	−82
	2/2	−69
	4/4	−47
	6/6	−66
10	1/1	−58
	2/2	−106
	4/4	−67
	6/6	−75

TABLE 5

Relative phases of potential energy density and one Cartesian component of kinetic energy density

Frequency (Hz)	Measurement location	Modulation frequency (Hz)	Probe axial direction	$\angle(\tilde{p}^2/\tilde{u}^2)$ (degrees) without panels	$\angle(\tilde{p}^2/\tilde{u}^2)$ (degrees) with panels
700	1	1	Vertical	3	−1
			Transversal	2	1
			Longitudinal	−3	1
		4	Vertical	17	−5
			Transversal	30	5
			Longitudinal	5	8
		8	Vertical	−35	−8
			Transversal	−162	13
			Longitudinal	−3	18
3900	1	1	Vertical	3	2
			Transversal	−3	2
			Longitudinal	−1	1
		4	Vertical	1	3
			Transversal	−1	4
			Longitudinal	1	3
		8	Vertical	−14	−2
			Transversal	15	3
			Longitudinal	1	3
3900	2	1	Vertical	4	—
			Transversal	−5	—
			Longitudinal	−3	—
		4	Vertical	−2	—
			Transversal	−6	—
			Longitudinal	−1	—
		8	Vertical	−36	—
			Transversal	−20	—
			Longitudinal	12	—

the intensity probe axis. The results obtained in one of the empty reverberant rooms, and in the same room when treated with a number of sound absorbent panels installed, are presented in Table 5. The additional damping is seen generally to reduce the phase differences.

6.3. ROOM DISSIPATION LOSS FACTORS

The reverberation times of the two reverberant rooms were independently determined and the resulting estimates of DLF were compared with those derived from the application of the two power injection methods (see Table 6).

6.4. ERROR ANALYSIS

A Monte Carlo distribution analysis of the sensitivity of the estimated DLF's and CLF's to error in measured data showed that equation (7b) was potentially the greatest source of error [10].

TABLE 6

A comparison of room loss factors estimated from energy decay and power input techniques

Frequency (Hz)	Reverberation time for room 2, T_2(s)	η_2 $=2{\cdot}2/fT_2$	η_2 Power injection method	η_2 Power modulation technique	Deviation* (dB)
700	2·15	1·46e − 3	5·43e − 4	2·30e − 3	2·0
2500	2·12	4·15e − 4	1·72e − 4	5·60e − 4	1·3
3900 (1/1)	1·64	3·44e − 4	1·40e − 4	3·12e − 4	−0·4
3900 (6/6)	1·64	3·44e − 4	1·40e − 4	4·42e − 4	1·1

* Deviation between values estimated from power modulation and from reverberation time.

7. DISCUSSION OF RESULTS

The results presented in Tables 1 and 2 indicate fair agreement between the estimates of DLF's and CLF's obtained by the steady state and modulated power injection techniques. It should, of course, be remembered that both sets of estimates are subject to uncertainty, no precise theoretical estimates being available.

The modulation phase dispersion phenomenon has also been observed by Lundberg [7, 8], which he characterizes as loss of spatial coherence of the modulation transfer function. As far as we are aware, this phenomenon has not been theoretically investigated (at the time of writing): this is clearly an urgent requirement, since the phenomenon appears to place considerable doubt on the validity of extension of the SEA equations to represent non-stationary vibrational energy flow between subsystems, especially in the case of impulsive excitation in which rapid rates of change of energy density and energy exchange occur. The observed differences between the modulation phases of kinetic and potential energy densities is particularly puzzling, since exchange between these components of energy density would be expected to take place on a time scale associated with the vibration frequency which is typically more than one hundred times the modulation frequency in the reported experiments.

As proposed by Lundberg [8], it is unnecessary to implement the input modulation by physical means: the process can be simulated computationally on the basis of measured impulse responses. It appears likely that such implementation, which avoids the complexity of the physical modulation process, together with its attendant time consumption and imperfections, is the appropriate way to proceed in future, and opens the way for application to multiple subsystem networks.

8. CONCLUSIONS

A procedure for determining the DLF's and CLF's of an SEA system by means of vibrational input modulation has been presented. The results compare reasonably well with those derived by application of the conventional steady state power injection techique. The principle advantages over the latter are that it is not necessary to quantify the input power, and, provided that reliable estimates of modal densities are available, response measurements are required only at one point on each subsystem. However, questions remain about the quality of numerical conditioning of the equations used to derive the loss factors, and the resulting sensitivity to errors in experimentally derived data is yet to be established. The current results indicate that accuracy is improved by injecting power sequentially into each subsystem in turn. Replacement of the reported physical input modulation procedure by computational simulation based upon measured impulse

responses offers the opportunity for further extensive research on the merits, or otherwise, of the modulation technique in application to complex practical systems.

A phenomenon of spatial dispersion of response energy modulation phase has been observed. Its physical origin and manifestation in spatially uniform and non-uniform subsystems urgently requires theoretical modelling and analysis, since it places in doubt the validity of extension of the SEA power balance equations to cases of transient excitation.

ACKNOWLEDGMENTS

We gratefully acknowledge the financial support for the M.Sc. studies of the second author provided by the Brazilian Navy and the Directorate of Naval Engineering. We are indebted to Karl-Ola Lundberg for generously sharing with us the results of his research after our parallel endeavours had become mutually evident. We also wish to acknowledge the vital contribution to the project made by Mr Rob Stansbridge and his colleagues in the electronic research and development secion of the ISVR.

REFERENCES

1. F. J. Fahy and P. P. James 1996 *Journal of Sound and Vibration* **190**, 363–388. A study of the kinetic energy impulse response as an indicator of the strength of coupling between SEA subsystems.
2. D. A. Bies and S. Hamid 1990 *Journal of Sound and Vibration* **70**, 187–204. *In-situ* determination of loss and coupling loss factors by the power injection method.
3. N. Lalor 1987 *ISVR Technical Report No*. 150, *University of Southampton*, *U.K*. The measurement of SEA loss factors on a fully assembled structure.
4. N. Lalor 1990 *ISVR Technical Report No*. 182, *University of Southampton*, *U.K*. Practical considerations for measurement of internal and coupling loss factors on complex structures.
5. K. de Langhe 1995 *Ph.D*. *Thesis*, *PMA Department*, *Katholieke Universiteit Leuven*, *Belgium*. High frequency vibrations: contribution to experimental and computational SEA parameter identification.
6. K.-O. Lundberg 1993 *Engineering Acoustics Report*, *Lund Institute of Technology*, *Lund*, *Sweden*. Modulation transfer function for estimation of loss factors in coupled systems.
7. K.-O. Lundberg 1994 *Proceedings of the Nordic Acoustical Meeting*, *Aarhus*, *Denmark*, 71–76. *In-situ* determination of coupling loss and loss factors in an SEA system consisting of two subsystems.
8. K.-O. Lundberg 1995 *Proceedings of the* 15th *International Congress on Acoustics*, *Trondheim*, *Norway*, 519–522. *In-situ* estimation of coupling loss and loss factors in an SEA-system using modulation transfer functions.
9. F. J. Fahy 1994 *ISVR Technical Report No*. 240, *University of Southampton*, *U.K*. Evaluation of SEA loss factors using input power modulation.
10. H. M. Ruivo 1995 *M.Sc*. *Dissertation*, *ISVR*, *University of Southampton*, *U.K*. *In-situ* evaluation of SEA loss and coupling loss factors between two subsystems by the power modulation technique.
11. F. J. Fahy 1969 *Journal of Sound and Vibration* **10**, 517–518. Measurement of mechanical input power to the structure.

APPENDIX: PRACTICAL IMPLEMENTATION OF THE POWER MODULATION TECHNIQUE

The technique of input power modulation will normally be applied to a band-limited random input force signal. However, in order to illustrate the principle of the technique, a single frequency input force will be assumed. Let the input force be expressed as

$$F(t) = F \cos \omega t \cos \Omega t = \tfrac{1}{2} F(\cos (\omega + \Omega)t + \cos (\omega - \Omega)t). \tag{A1}$$

Let $\omega + \Omega = \omega_1$ and $\omega - \Omega = \omega_2$. Assume the force to be applied to a subsystem having complex point mobilities $\tilde{Y}(\omega_1)$ and $\tilde{Y}(\omega_2)$ at these frequencies. The instantaneous power input is given by

$$\begin{aligned} P(t) = \tfrac{1}{4} F^2[& Y_R(\omega_1)\,(\cos^2\omega_1 t + \cos\omega_1 t \cos\omega_2 t) \\ & - Y_I(\omega_1)\,(\cos\omega_1 t \sin\omega_1 t + \sin\omega_1 t \cos\omega_2 t) \\ & + Y_R(\omega_2)\,(\cos^2\omega_2 t + \cos\omega_1 t \cos\omega_2 t) \\ & - Y_I(\omega_2)\,(\cos\omega_2 t \sin\omega_2 t + \cos\omega_1 t \sin\omega_2 t)], \end{aligned} \tag{A2}$$

where $\tilde{Y} = Y_R + iY_I$. Averaging $P(t)$ over an interval of time which is long compared with $2\pi/\omega_1$ and $2\pi/\omega_2$, but short compared with $2\pi/\Omega$, yields the approximate expression for the "smoothed" input power:

$$\langle P \rangle \approx \tfrac{1}{8} F^2\{[Y_R(\omega_1) + Y_R(\omega_2)]\,[1 + \cos 2\Omega t] - [Y_I(\omega_1) - Y_I(\omega_2)]\,[\sin 2\Omega t]\}. \tag{A3}$$

The ratio of the average value of the Y_I difference to the average value of Y_R sum over a band of frequency containing a number of modal resonances will normally be much less than unity, and the second product will be negligible. Equation (A3) is therefore a good approximation to the desired form of equation (2): hence, full wave modulation of the imput force at frequency Ω will produce the desired form of input. The smoothed quantities may be obtained by passing the input and response signals through a squaring circuit followed by a smoothing circuit.